PAPER

Early damage detection in epoxy matrix using cyclobutane-based polymers

IOP Publishing Smart Materials and Structures
Smart Mater. Struct. **23** (2014) 095038 (10pp) doi:10.1088/0964-1726/23/9/095038

Early damage detection in epoxy matrix using cyclobutane-based polymers

Jin Zou, Yingtao Liu, Bohan Shan, Aditi Chattopadhyay and Lenore L Dai

School for Engineering of Matter, Transport, and Energy Arizona State University, Tempe, AZ 85287, USA

E-mail: Lenore.Dai@asu.edu

Received 9 April 2014, revised 16 June 2014
Accepted for publication 26 June 2014
Published 15 August 2014

Abstract

Identification of early damage in polymer composites is of great importance. We have incorporated cyclobutane-containing cross-linked polymers into an epoxy matrix, studied the effect on thermal and mechanical properties, and, more importantly, demonstrated early damage detection through mechanically induced fluorescence generation. Two cinnamate derivatives, 1,1,1-tris(cinnamoyloxymethyl) ethane (TCE) and poly(vinyl cinnamate) (PVCi), were photoirradiated to produce cyclobutane-containing polymer. The effects on the thermal and mechanical properties with the addition of cyclobutane-containing polymer into epoxy matrix were investigated. The emergence of cracks was detected by fluorescence at a strain level just beyond the yield point of the polymer blends, and the fluorescence intensified with accumulation of strain. Overall, the results show that damage can be detected through fluorescence generation along crack propagation.

Keywords: cyclobutane, stress-strain, crack sensor

(Some figures may appear in colour only in the online journal)

1. Introduction

Material degradation caused by mechanical deformation, thermal expansion/contraction, radioactive contamination, chemical corrosion, or electrical discharges occurs inevitably in practical applications and significantly reduces material performance, especially in harsh environments [1–4]. For example, aerospace materials are exposed to large changes in pressure, temperature, speed, and other elements. All these elements can cause large accumulations of stresses on the materials [5]. Beyond a certain threshold, microscopic cracks begin to form and grow irreversibly, and they eventually result in complete destruction of the materials and jeopardize public safety [6–8]. It is of great importance to monitor the health conditions of materials in service; in this way, people can take steps before materials reach mechanical failure.

Scientists have studied many years to develop damage detection technology. Recent research has shown that the use of electromechanical (E/M) impedance methods allows for the direct identification of structural dynamics [9–11]. The mechanism is to couple small-size piezoelectric active sensors, such as lead zirconate titanate, with the material structure. The measurements of the E/M impedance or admittance signatures are related to mechanical impedance, which is affected by the presence of damage. The Lamb wave method is also suitable for structural health monitoring applications [12, 13].

Damage in a structure can also be by identified by using a self-monitoring means such as crack sensors. Several types of crack sensors have been developed in recent years [14–16]. In particular, with a view to ease of detection, a great deal of effort has been devoted to developing methods of detecting damage in terms of visibility. A visible color change can indicate areas under stress and provide a signal if damage has occurred. Mechanofluorochromic materials, which depend on changes in physical molecular packing modes in response to mechanical stimuli, can be used as stress sensors [17–19]. Crenshaw *et al*, as pioneers in organic mechanofluorochromism, demonstrated that tensile deformation can facilitate substantial changes in the luminescent properties of linear low-density polyethylene (LLDPE)–dye blends by the destruction of dye aggregates [19]. The deformation color can be tuned by varying the electronic molecular structures of the dye molecules. However, the limited solubility of organic dye in a polymer matrix limits the application of this system in some materials. Materials that respond to external stress with

a color change are already known, but most color change processes are activated by the disruption or formation of non-covalent bonds. Mechanophores, force-sensitive molecular units, give visible color change upon the scission of covalent bonds in a structure. In recent years, mechanophore-linked polymers have attracted significant interest because they expand the scope of applications in that a variety of polymers become accessible. Sijbesma *et al* synthesized stress-sensitive polymer by incorporating the bis(adamantly)-1,2-dioxetanes unit, which enables transduction of force into a temporal visible luminescence under stress via opening of the four-membered dioxetane ring with subsequent ketone product relaxation from its excited state to the ground state [20]. Pyran-based organic compounds, such as spiropyrans, spirooxazines, and naphthopyrans, are well-known chromogenic materials for which structure changes occur in conjunction with a color change induced by temperature or light [21–24]. However, color change induced by external force in pyran-based compounds has not been extensively reported. Davis *et al* synthesized spiropyran-linked elastomeric polymers, which were able to act as a force sensor in response to stress loading [25]; this response was accompanied by a color change through a mechanically induced 6-electrocyclic ring-opening reaction from colorless spiropyran to colored merocyanine conformations.

Although mechanophore-linked polymer has provided tremendous new opportunities, especially in the areas of stress sensing and early crack/failure detection, many unknown fundamentals as well as unexplored applications remain. Current research gives greater emphasis to pure and bulk traditional polymers; synthesis relies solely on an individual chemistry/reaction mechanism that is often limited and complicated. Here we have designed and synthesized a mechanically responsive composite material system by blending cyclobutane-containing polymer into an epoxy matrix to identify the location of damage through mechanically induced fluorescence generation.

2. Methodology

2.1. Materials

Unless otherwise stated, all the following listed materials and reagents were used as received. 1,1,1-tris(hydroxymethyl) ethane (99%), cinnamoyl chloride (98%), tetrahydrofuran (⩾99.9%), 4-(dimethylamino)pyridine (⩾99%),dichloromethane (⩾99.8%), ethanol (⩾99.5%), and poly(vinyl cinnamate) (PVCi, average M_n 45 000–55 000) were purchased from Sigma-Aldrich. Sodium chloride (⩾99%) and water (HPLC) were purchased from Fisher Scientific. Epoxy resin FS-A23 (digycidylether of bisphenol F, DGEBPF) and epoxy hardener FS-B412 (diethylenetriamine, DETA) were purchased from Epoxy System Inc.

2.2. Synthesis of 1,1,1- tris (cinnamoyloxymethyl) ethane (TCE)

TCE was prepared through the reaction between 1,1,1s-tris (hydroxymethyl)ethane and cinnamoyl chloride [26]. The crude product was purified by recrystallization through hot ethanol. ^{1}H and ^{13}C nuclear magnetic resonance (NMR) spectra were taken using a Bruker 400 MHz NMR spectrometer. The ^{1}H NMR ($CDCl_3$) data for TCE are as follows: δ1.178 (s, 3 H, CH_3), 4.292 (s, 6 H, OCH_2), 6.442 (d, 3 H, J = 16 Hz, phCH), 7.260–7.504 (m, 15 H, phenyl), 7.688 (d, 3 H, J = 16 Hz, phCH), ^{13}C NMR ($CDCl_3$): δ17.402 (CH_3), 38.839 (CCH_3), 66.282 (OCH_2), 117.544, 128.173, 128.895, 134.209 (phenyl), 130.435 (phCH), 145.411 (phCH = CH), 166.699 (carbonyl). Mass spectra were conducted using a JEOL LCMate mass spectrometer. The calculated molecular mass for TCE is 511.2205, and [M-H] at 510.2042 was detected experimentally.

2.3. Preparation of cyclobutane-containing polymer and polymer blends

To prepare TCE polymer or PVCi polymer, solid TCE or PVCi was first dissolved in CH_2Cl_2. The solution was applied on a clean silicon mold to form a thin film and placed in a vacuum to evaporate the excess CH_2Cl_2. After the evaporation of the CH_2Cl_2, the thin film was photoirradiated at 302 nm for 4 h. All the silicon molds and glass slides used for preparation of samples were pretreated with a mold release agent.

To prepare polymer/epoxy polymer blends, the TCE or PVCi solution was added to DGEBPF and thoroughly dispersed by using an ultrasonic probe sonicator (Sonics VibraCell, 500 W model) for 20 s. The mixture was placed in a vacuum chamber at 50 °C to evaporate the CH_2Cl_2 until the mass of the mixture remained unchanged, indicating that the excess CH_2Cl_2 had evaporated. The resin mixture was cooled to room temperature before DETA was added and mixed (M_{TCE} or $_{PVCi}$: M_{Epoxy} = 1:10; M_{DGEBPF}: M_{DETA} = 100:27). The mixture was sonicated in an ice bath to prevent any premature curing. After the mixture became homogenous, the mixture was poured into the silicon molds and moved into a vacuum chamber to degas for 30 min, followed by photo-irradiation conducted by a UV lamp of 302 nm wavelength (UVP, UVM-28). According to the manufacturer's data, the light density was approximately 1300 μW cm^{-2} at a distance of 3 cm. The sample was exposed to UV for 4 h and cured overnight at room temperature in atmosphere. A neat epoxy sample followed a similar procedure for comparison. After simple machining, the sample was ready for test. The average dimension of the cubic sample was 3 × 4 × 8 mm.

2.4. Characterization of photochemical properties of cinnamates

All UV spectroscopic analyses were performed using a UV–Vis spectrometer (Perkin Elmer Lambda 18). The spectra of the samples were recorded before exposure and after each exposure at selected intervals of time. All measurements were

performed using the same parameters at room temperature. The FT-IR spectra were analyzed using a Bruker IFS 66 V S^{-1} FTIR spectrometer. TCE was dissolved in CH_2Cl_2 and was spread out on a KBr disk and left without any disturbance. CH_2Cl_2 was then evaporated off in a vacuum oven at room temperature to form a very thin film.

2.5. Characterization of polymer blends

The measurements of T_g were carried out by differential scanning calorimeter thermal analysis (DSC). Experiments were performed in a nitrogen atmosphere using TA Instruments Q20. Throughout the DSC work, temperature and heat flow calibrations were performed following standardized procedures. After a heating and cooling cycle up to 70 °C with a heating ramp rate of 10 °C min^{-1} to eliminate thermal history, T_g was analyzed from the data of the second heating scan from −20 to 120 °C at 10 °C min^{-1}, using TA universal Analysis software. All samples were contained in Tzero pans with lids. An empty pan with a lid was used for reference. Thermogravimetric analysis (TGA) was carried out using a TA Instruments (TGA Q500) machine. The sample was placed in a tared platinum crucible. All the samples were heated from 30 to 600 °C at a heating rate of 10 °C min^{-1} in nitrogen. The compressive stress-strain curves of these systems were obtained by conducting tests on an MTS servo hydraulic test system. The tests were run in displacement control in the longitudinal direction at a loading rate of 1 mm min^{-1}. To monitor the fluorescence generation from cracked polymer blends, the cubic samples of the polymer blends were compressed to different strains and observed simultaneously under a fluorescence microscope (Nikon Eclipse TE300 inverted video microscope) by exposure to 330–380 nm UV light.

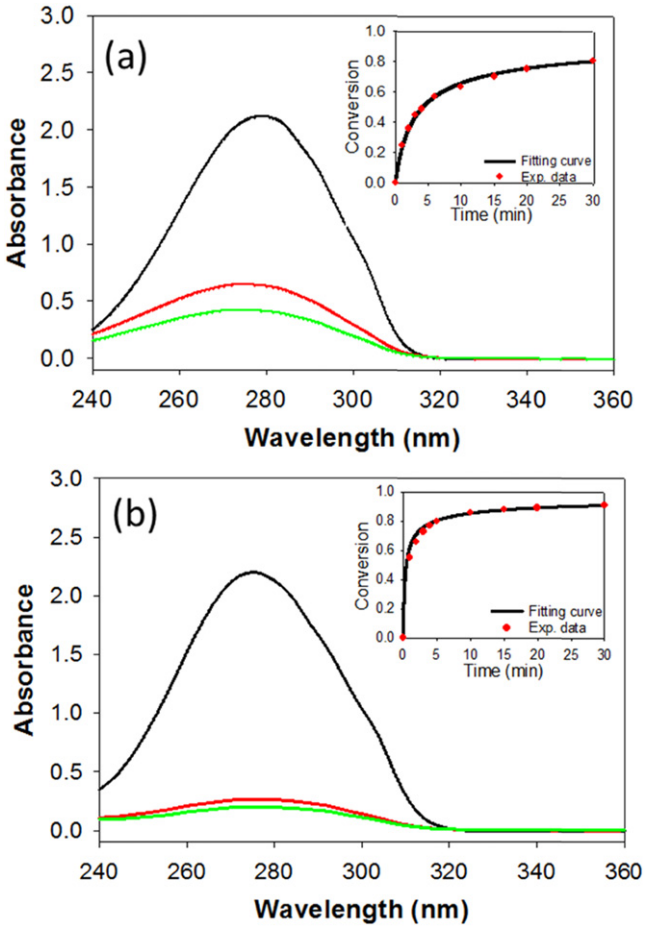

Figure 1. The change in UV absorbance of (a) TCE and (b) PVCi solution as a function of UV exposure time (—0 min; —15 min; —30 min). The inset figures provide the change in the conversion as a function of the UV exposure time.

3. Results and discussion

3.1. Photoreaction of TCE and PVCi

In our study, we applied epoxy as the matrix material. Epoxies are among the most popular thermosetting polymers and are widely used in the automobile, aircraft, sports equipment, and other industries due to their excellent mechanical performance, thermal stability, and flame retardancy [27–30]. Cyclobutane was applied into the epoxy as mechanophores: 1,1,1-tris(cinnamoyloxymethyl) ethane (TCE) was dimerized through [2 + 2] cycloaddition into a cyclobutane ring under photoirradiation to eventually form a three-dimensional network. This cyclic product has been proved to efficiently generate fluorescence emission upon cleavage of the cyclobutane ring [31]. The [2 + 2] photocycloaddition of the cinnamoyl groups was analyzed using both UV–vis and FTIR spectroscopy. Figure 1(a) displays the variation in UV absorbance of TCE dilute solution as a function of UV exposure time. The solution exhibited strong UV absorbance between 250 and 350 nm with a peak centered at approximately 280 nm; this likely corresponds to the abundance of π-π^* transitions of the C=C double bond from cinnamoyl groups before photoirradiation, as reported elsewhere [26, 32, 33]. The change in the absorbance value was monitored by continual irradiation, and it was obvious that the absorbance band decreased rapidly with exposure time and disappeared almost completely within 30 min of photoirradiation. This observation implies the formation of cyclobutane. The spectra underwent a slight blue shift from 280 to 272 nm due to the change in chemical structure of the cinnamate groups under photoirradiation. For comparison, we also purchased PVCi, which has the cinnamate functional group as side groups of the polymer chain, to produce cyclobutane upon photoirradiation. PVCi is prominent in photochemistry, with certain attractive characteristics [34–36]. The UV absorbance of the PVCi dilute solution exhibited a trend similar to that of the TCE solution upon photoirradiation, as shown in figure 1(b). Cycloaddition efficiency can be calculated according to the rate of disappearance of the C=C double bond of the cinnamoyl group by using the following equation: conversion (%) = $(A_0 - A_t)/A_0 \times 100$, where A_0 is the absorbance before irradiation at the maximal wavelength and A_t is the corresponding absorbance during photoreaction [37]. The conversion as a function of

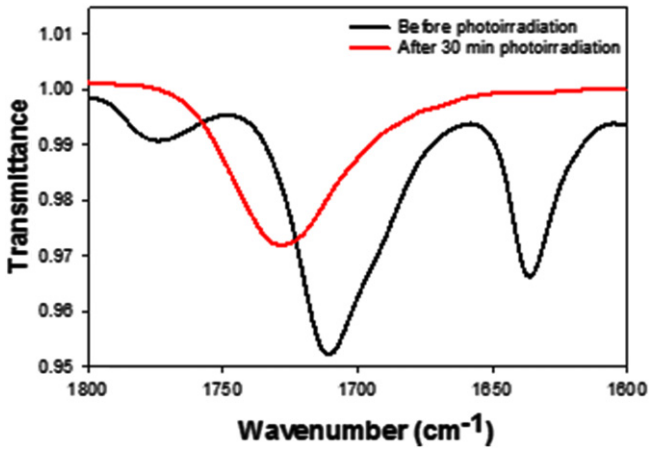

Figure 2. IR spectra of TCE film on a KBr disk before and after photoirradiation.

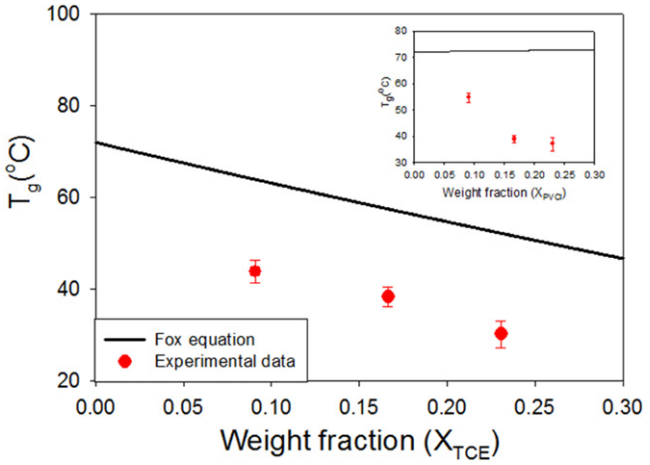

Figure 4. Comparisons of theoretical and experimental T_g of epoxy with various contents of TCE polymers and PVCi polymers (inset).

time is plotted in figure 1 (inset) and estimated to be over 80% and 90% based on the absorbance change at 280 nm after 30 min of UV exposure. In addition, it was observed from both plots that conversion (%) never reached 100%. This can be explained by steric hindrance from formation of the polymer network.

Results from FTIR were also used to track the transformation of the functional groups during photoirradiation. Figure 2 shows the FTIR spectra of the TCE film before and after irradiation under UV light. The peaks at 1713 cm^{-1} and 1637 cm^{-1} corresponded to the conjugated C=O stretching vibration and vinylene C=C stretching vibration, as reported elsewhere [33, 38]. After 30 min of photoirradiation, the C=C peak disappeared due to consumption in forming cyclobutane by photo-dimerization, which destroyed the conjugation in the entire π-electron system. The C=O peak shifted to a higher wavenumber with decreasing absorbance; this may be attributed to the loss of π–conjugation from the C=C double bond [38, 39].

3.2. Effects of addition of polymers to the thermal and mechanical properties of polymer blends

Subsequently, we incorporated cyclobutane-containing polymers into an epoxy matrix and first studied glass transition temperatures (T_g). Polymer blending was recognized as a common way to develop new materials. Appropriate blending can offer useful extended properties compared with neat properties. However, immiscibility and incompatibility are the main problems for most polymer blends and limit their usefulness in practical application. Fully miscible blends are characterized by a single glass transition temperature, unaffected by the number of polymer components the blends contain [40]. In contrast, immiscible blends for binary components usually have two glass transition temperatures. The DSC curves of the neat epoxy and polymer blends are displayed in figure 3. Only one glass transition temperature was observed for polymer blends, suggesting that the epoxy- and cyclobutane-containing polymers were quite miscible with

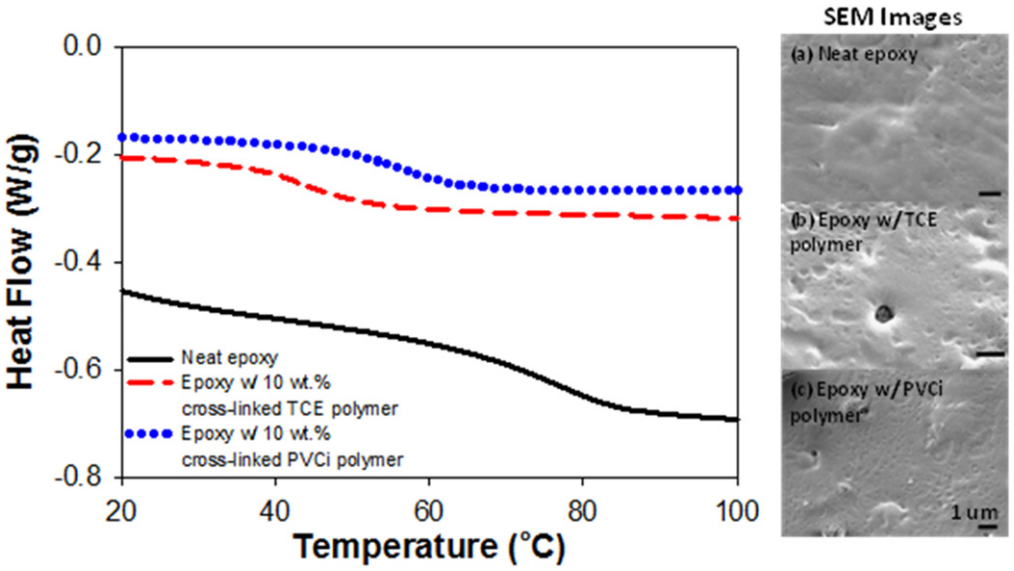

Figure 3. DSC curves and SEM images for neat epoxy and epoxy/polymer blends: (a) neat epoxy (b) epoxy with10 wt.% TCE polymer (c) epoxy with 10 wt.% PVCi polymer.

each other. The miscibility of the blends was further confirmed by scanning electron microscopy (SEM), in which no noticeable phase separation was detected.

It has been reported that the T_g of epoxy polymer blends may vary due to different factors such as compositions of the blends or the conversion of the curing reaction [41–43]. The T_gs of the neat polymer and polymer blends are summarized in table 1. The addition of TCE polymers or PVCi polymers to epoxy significantly changed the glass transition temperature. For a binary system, the T_g of the system can be calculated by the Fox equation $\frac{1}{T_g} = \frac{x_1}{T_{g,1}} + \frac{1-x_1}{T_{g,2}}$, where $T_{g,i}$ is the glass transition temperature of component i and x_i is the mass fraction of component i [40]. The comparisons between the experimental and calculated values are shown in figure 4. Theoretically, the glass transition temperature of the epoxy with TCE polymers deceases with the addition of TCE polymers, whereas the glass transition temperature of the epoxy with PVCi polymers increases with the addition of PVCi polymers, due to the lower T_g of TCE polymers and higher T_g of PVCi polymers than neat epoxy. Obviously, the measured values of the samples deviated significantly from the theoretical values. _ENREF_41We hypothesize that the photocycloaddition of TCE or PVCi reduced the curing degree of epoxy significantly. The cross-linking reaction in neat epoxy was that the nucleophilic amine in the DETA attacked the carbon atom in the ethylene oxide ring to form a C-N bond [44]. TCE or PVCi introduced an additional carbonyl group into the blends, which might have influenced the cross-linking process of epoxy due to the possible interactions between the carbonyl group and the amine. In addition, the low cross-linking of epoxy could have been caused by network formation via the cycloaddition of cinnamates, which restrained the motion and the rotation of resin and hardener monomers during the curing process. Therefore, the addition of more polymers would make the T_g much lower.

Thermogravimetric analysis (TGA) was used for characterizing the thermal stability of the TCE polymers, PVCi polymers, and polymer blends. Weight loss due to thermal degradation is an irreversible process and is closely related to oxidation through the interaction between the molecular bonds of a polymer and oxygen molecules [45–47]. Besides oxidation, polymers can be thermally degraded by random chain scission, side-group elimination, and so on [48, 49]. Because we ran all TGA measurements under nitrogen in our experiment, thermal degradation by oxidation was eliminated. The TGA and differential thermal gravimetry (DTG) curves as a function of temperature for TCE polymer and PVCi polymer are shown in figure 5(a). The peak of the DTG (T_p) indicated the point of greatest rate of change on the weight loss curve. Obviously, the TCE polymer showed a higher initial decomposition temperature, which started at 250 °C and completed at 430 °C. Thermal decomposition of the PVCi polymer occurred at 100 °C. According to the DTG curve, the TCE polymer had a single major decomposition step; the PVCi polymer had two subsequent major decomposition steps separated by a transition region corresponding to the decomposition of cyclobutane and the polyvinyl backbone [50].

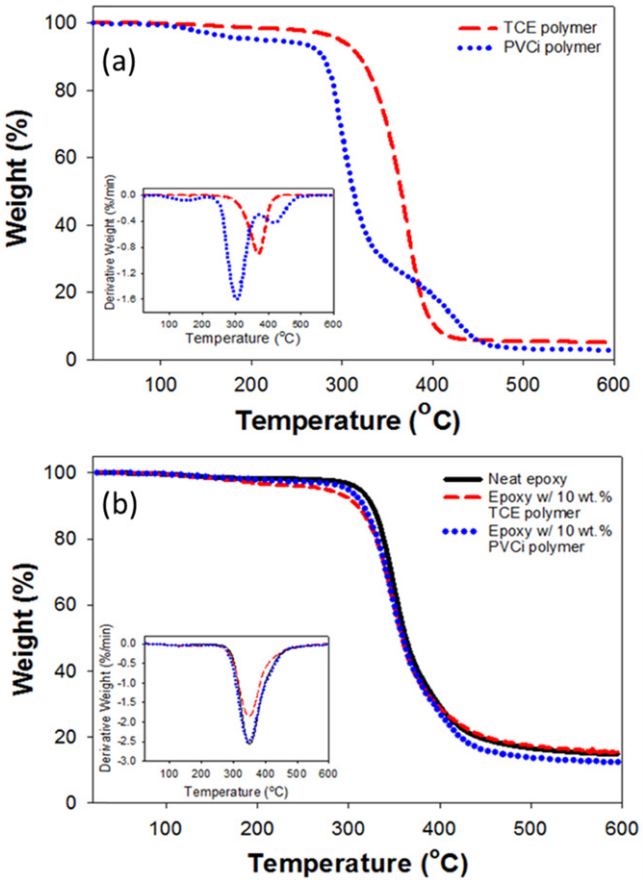

Figure 5. TGA and DTG curves (insets) of (a) TCE and PVCi polymers; (b) neat epoxy and polymer blends.

Table 1. T_g of polymer and polymer blends.

	Neat epoxy	TCE polymer	PVCi polymer	Epoxy w/ (10, 20, 30) wt.% TCE polymers	Epoxy w/ (10, 20, 30) wt.% PVCi polymers
Tg, °C	72	0	75	44, 38, 29	55, 40, 36

The TGA and DTG curves of neat epoxy and polymer blends are displayed in figure 5(b). Single-step decomposition was observed in all samples. The addition of TCE polymer or PVCi polymer increased the onset of thermal decomposition of epoxy slightly. According to the DTG curve, the derivative value for epoxy with PVCi polymer was higher than that of epoxy and epoxy with TCE polymer. The T_p and the corresponding weight loss are summarized in table 2. The data indicated that the addition of polymer increased the rate of degradation of epoxy, which could be attributed to the weaker cross-linking of epoxy.

Stress-strain curves of the neat epoxy and epoxy and polymer blends were determined in compression tests, as shown in figure 6. The strain (%) was calculated from the ratio of displacement to the initial dimension. All three systems displayed a qualitatively similar stress-strain behavior.

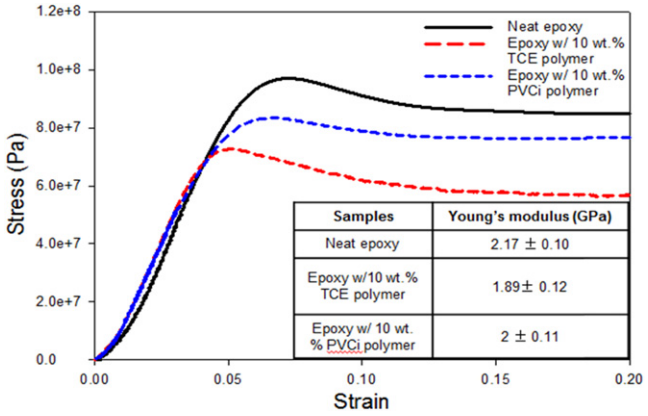

Figure 6. Compressive stress-strain curves for the pure epoxy and epoxy w/ 10 wt.% TCE polymers and PVCi polymers dispersed in the matrix. The inset table is the summary of Young's modulus of samples.

The curves exhibited an initial linear elastic response followed by yielding. With a slow drop-off in stress, a plateau region was observed for a wide range of strains. Young's modulus for neat epoxy and polymer blends was determined by a linear regression to the slope of the stress-strain curve in the initial linear elastic region and summarized in figure 6 (inset table). Young's modulus was comparable for neat epoxy and polymer blends. Young's modulus for higher-concentration TCE polymer blends (20% TCE) was calculated as 1.6 GPa, much lower than for the neat epoxy. The neat epoxy exhibited higher yield stress than the two polymer blend systems, revealing that the ability of the epoxy system to resist damage declined with the addition of TCE polymers or PVCi polymers. On the other hand, neat epoxy is advantageous regarding application of a crack sensor because polymer blends may be more sensitive and deform more easily under stress.

Table 2. T_p and the corresponding weight loss of polymer and polymer blends in TGA analysis.

	Neat epoxy	TCE polymer	PVCi polymer	Epoxy w/10 wt. % TCE polymers	Epoxy w/10 wt. % PVCi polymers
T_p, °C	347	373	298 419	357	357
weight loss, %	31.1	61.4	30.4 86.3	47.9	47.9

3.3. Fluorescence response by mechanical activation

The goal for the application of cyclobutane-containing polymers in the solid state here was to demonstrate mechanochemical cleavage of a covalent bond, and further to investigate the use of these cyclobutane-containing polymers blended with epoxy as stress/strain or damage sensors by visual detection. It is well known that force distribution is not uniform throughout a material under stress. Force distribution is dependent on coupling between macroscopic forces and molecular forces. The spectroscopic signal can be measured and imaged to quantify the force.

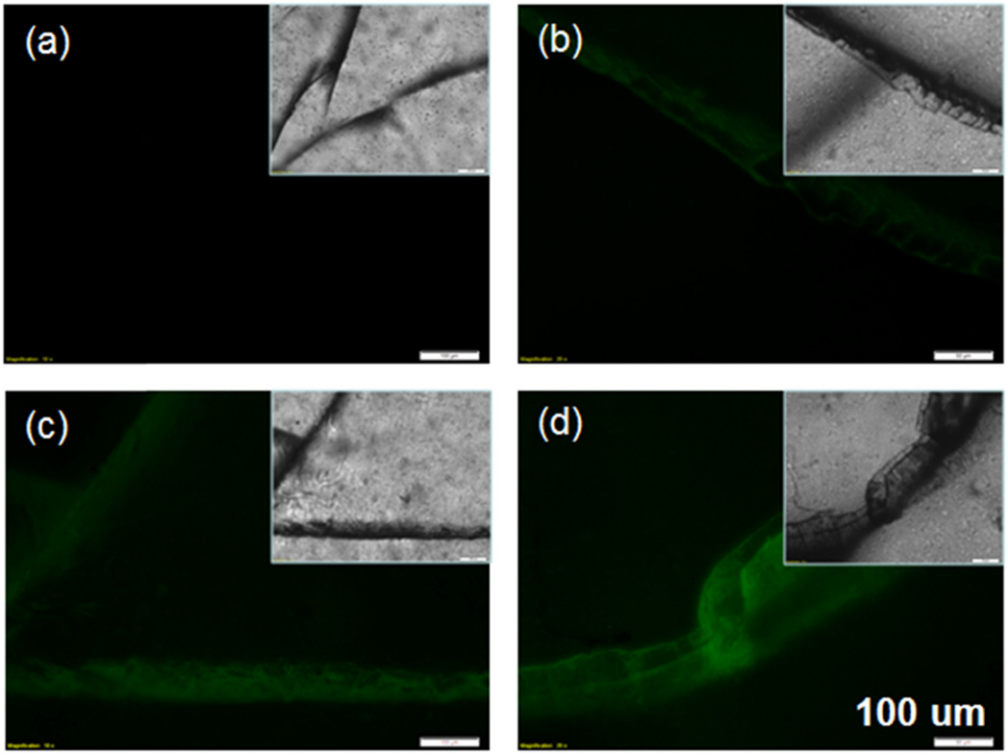

Figure 7. Microscopic images of fluorescence emission along cracks generated by hammer smash on polymer blends (a) without and (b) with 10 wt.%, (c) 20 wt.%, and (d) 30 wt.% TCE polymers. The insets are the corresponding images under white light.

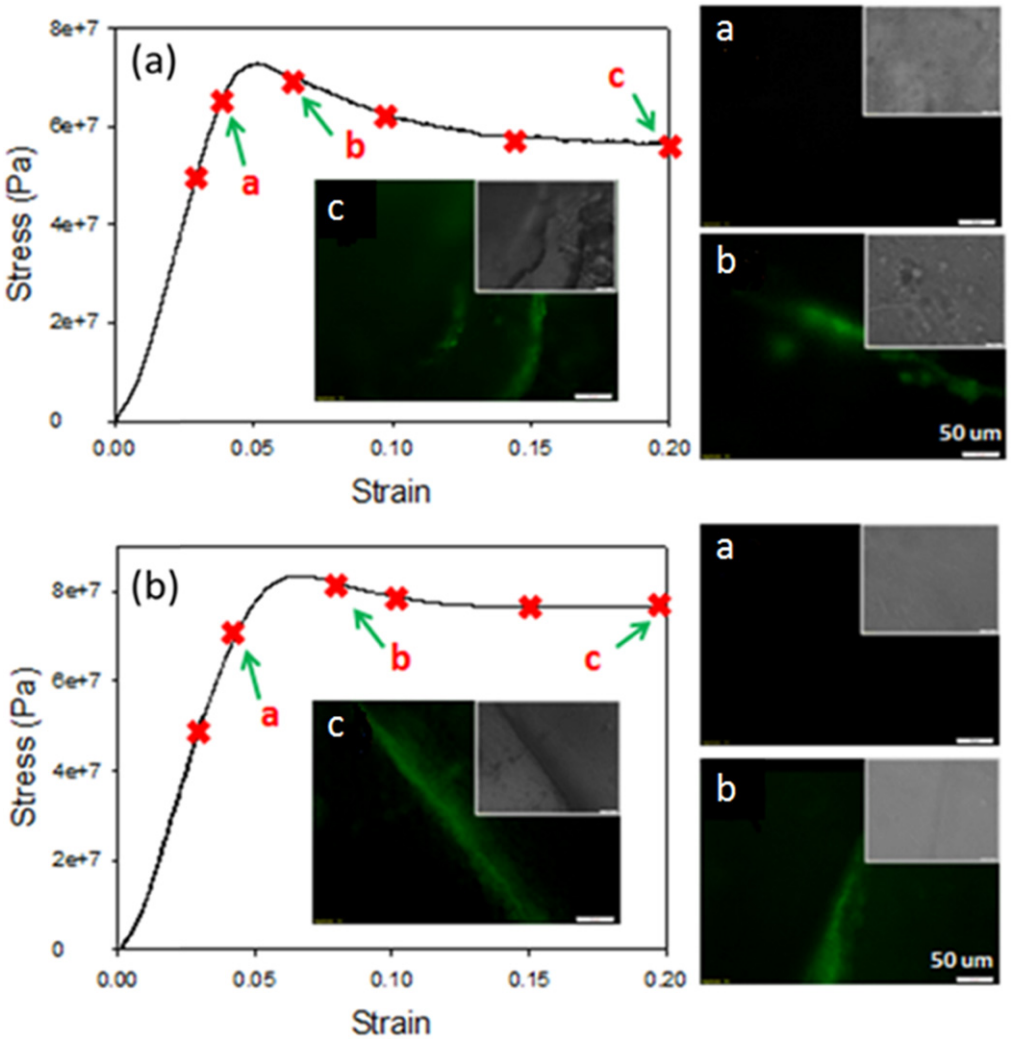

Figure 8. Microscopic images of fluorescence emission of (a) epoxy w/ 10 wt.% TCE polymers and (b) epoxy w/ 10 wt.% PVCi polymers at different strains.

Cracks were first generated by hammer smash on the neat epoxy and polymer blends. For neat epoxy, the cracks were observed under white light only; nothing was detected under UV light, as displayed in figure 7(a). Fluorescence emission along the cracks was clearly observed in figure 7(b) under UV light when epoxy was blended with 10 wt.% TCE polymers, confirming that the fluorescence was due to the incorporation of TCE polymers. Cyclobutane is a four-membered ring molecule known for its highly strained structure, largely attributed to angle strain and torsional strain [51]. The mechanically induced cleavage of the C-C bonds of cyclobutane was thus relatively easy. It implied that, in the polymer blends, the cleavage of cyclobutane was the major reaction under stress because the C-C bond in cyclobutane was much weaker than the bonds in the epoxy polymer structure. The corresponding images of epoxy with 20 wt.% and 30 wt.% TCE polymers are displayed in figures 7(c) and (d). As the images show, the fluorescent signal was further augmented with the increase in the amount of TCE polymers blended with the epoxy, implying that more mechanically induced reactions in cyclobutane occurred under stress. From the images, it can be seen that epoxy with 10 wt.% TCE polymer provided sufficient fluorescent emission to detect damage. Thus, the content of 10 wt.% was used for the subsequent fluorescent tests.

In a compression test on epoxy with 10 wt.% TCE polymers, the fluorescent signal was monitored at six points on the stress-strain curve, as shown in figure 8(a). The evolution of induced fluorescence emission for the polymer blends is displayed through representative images at point (a) (immediately before the yield point), point (b) (immediately after the yield point), and point c (with strain of 20%). No obvious fluorescence was observed before the yield point was reached; immediately after the yield point, micro-cracks were observed under UV by fluorescence emission, whereas they were not observed under white light, indicating that the fluorescence emission was able to provide higher sensitivity to and easy detection of the location of cracks, especially for early damage detection, even though the initiation of crack formation usually goes unnoticed under white light. It was also noted that fluorescence emission along the crack intensified with strain after the yield point. The compression test

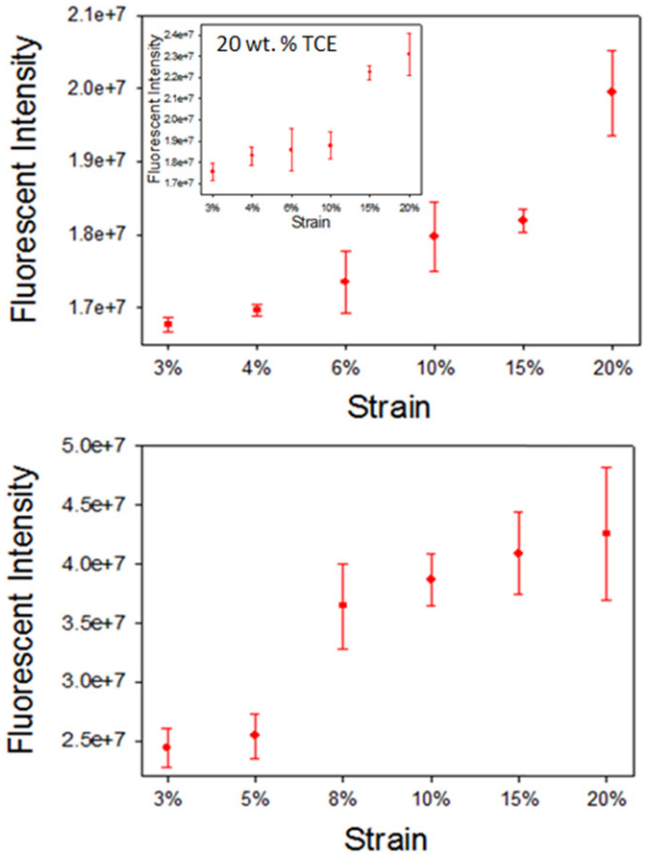

Figure 9. Integrated density of fluorescence emission in response to different strains of epoxy w/ 10 wt.% (top) TCE polymers (the inset is 20% wt.% TCE) and (bottom) PVCi polymers.

was conducted on epoxy with 10 wt.% PVCi polymers. Both polymer blends displayed similar behavior with respect to fluorescent response under stress. Molecular architecture is important for force transfer through bulk material to a cleavable bond in a mechanophore. The TCE had three cinnamate functional groups in each molecule, and the cycloaddition of cinnamates led to the formation of a three-dimensional network; the PVCi had multiple cinnamate functional groups as the chain side that connected the polyvinyl chain into a network through cyclobutane acting as a cross-linker. In the compression test, both polymer structures enabled efficient transfer of mechanical force through bulk epoxy matrix to achieve a mechanochemical reaction in cyclobutane, thereby inducing fluorescence generation. For comparison, a tensile test was conducted on polymer blends. Polymer blends tested under tension failed in a brittle manner, and no visual fluorescence was detected before failure or at the fracture surface after failure.

To further explore the relationship between the strains and their corresponding fluorescence response, ten fluorescent micrographs at each point were processed by ImageJ. The integrated intensity was calculated through the sum of pixel values in the image. The density at each point was averaged and plotted as a function of strain, as shown in figure 9. The onset of activation was observed below 6% strain and 8% strain (just past the yield point) for epoxy with TCE polymers and epoxy with PVCi polymers, respectively. The density increased with the accumulation of strain, which indicated that the activation of cleavage of cyclobutane was achieved at low strain and more activations occurred with mechanical loading. Epoxy with 20 wt. % TCE polymers (figure 9, top (inset)) displays a similar tendency, in which fluorescent intensity increases with strain.

4. Conclusion

We studied the effect on the thermal properties and mechanical properties of the addition of cyclobutane-containing cross-linked polymer into an epoxy matrix. The cross-linked TCE and PVCi polymers were both thermally stable for a wide range of temperature. The DSC experiment showed that the addition of cross-linked TCE and PVCi polymer shifted the glass transition temperature (T_g) to lower temperatures, likely due to a lower cross-linking degree of epoxy. In the compression test, the emergence of cracks was detected by fluorescence at a strain level just beyond the yield point of the blended polymer system, and the fluorescence intensified with accumulation of strain. The fluorescence provided greater sensitivity for visual detection compared with observation by white light. Moreover, the possibilities of multiple stress sensors mechanically activated at different levels that can be blended together as a more complex mechanophore combination will be an exciting undertaking.

Acknowledgments

We acknowledge the financial support of the Air Force Office of Scientific Research, grant number FA9550-12-1-0331, and Program Manager Dr David Stargel.

Reference

[1] Dasgupta A and Pecht M 1991 Material failure mechanisms and damage models *IEEE Trans. Reliab.* **40** 531–6
[2] Sih G C and Tang X S 2008 Micro/macro-crack growth due to creep-fatigue dependency on time-temperature material behavior *Theor. Appl. Fract. Mech.* **50** 9–22
[3] Kwon J D, Park J C, Lee Y S, Lee W H and Park Y W 2000 An investigation of the degradation characteristics for casting stainless steel, Cf8m, under high temperatures *Nucl. Eng. Des.* **198** 227–40
[4] Drummond J L 2008 Degradation, fatigue, and failure of resin dental composite materials *Journal of Dental Research* **87** 710–9
[5] John R, Jata K V and Sadananda K 2003 Residual stress effects on near-threshold fatigue crack growth in friction stir welds in aerospace alloys *Int. J. Fatigue* **25** 939–48
[6] Farrar C R and Worden K 2007 An introduction to structural health monitoring *Philosophical Transactions of the Royal Society a-Mathematical Physical and Engineering Sciences* **365** 303–15
[7] Ortiz M 1988 Microcrack coalescence and macroscopic crack-growth initiation in brittle solids *Int. J. Solids Struct.* **24** 231–50

[8] Ritchie R O 1999 Mechanisms of fatigue-crack propagation in ductile and brittle solids *Int. J. Fract.* **100** 55–83
[9] Giurgiutiu V and Zagrai A 2005 Damage detection in thin plates and aerospace structures with the electro-mechanical impedance method *Structural Health Monitoring-an International Journal* **4** 99–118
[10] Hamzeloo S R, Shamshirsaz M and Rezaei S M 2012 Damage detection on hollow cylinders by electro-mechanical impedance method: experiments and finite element modeling *Comptes Rendus Mecanique* **340** 668–77
[11] Zagrai A N and Giurgiutiu V 2001 Electro-mechanical impedance method for crack detection in thin plates *J. Intell. Mater. Syst. Struct.* **12** 709–18
[12] Kessler S S, Spearing S M and Soutis C 2002 Damage detection in composite materials using lamb wave methods *Smart Materials & Structures* **11** 269–78
[13] Monnier T 2006 Lamb waves-based impact damage monitoring of a stiffened aircraft panel using piezoelectric transducers *J. Intell. Mater. Syst. Struct.* **17** 411–21
[14] Zhang Y 2005 *Piezoelectric Paint Sensor for Real-Time Structural Health Monitoring Proc. SPIE* **5765** 1095–103
[15] Ali R, Mahapatra D R and Gopalakrishnan S 2005 Constrained piezoelectric thin film for sensing of subsurface cracks *Smart Mater. Struct.* **14** 376–86
[16] Rattanachan S, Miyashita Y and Mutoh Y 2005 Fabrication of piezoelectric laminate for smart material and crack sensing capability *Science and Technology of Advanced Materials* **6** 704–11
[17] Pucci A, Di Cuia F, Signori F and Ruggeri G 2007 Bis (benzoxazolyl)stilbene excimers as temperature and deformation sensors for biodegradable poly(1, 4-butylene succinate) films *J. Mater. Chem.* **17** 783–90
[18] Chi Z G, Zhang X Q, Xu B J, Zhou X, Ma C P, Zhang Y, Liu S W and Xu J R 2012 Recent advances in organic mechanofluorochromic materials *Chemical Society Reviews* **41** 3878–96
[19] Crenshaw B R, Burnworth M, Khariwala D, Hiltner A, Mather P T, Simha R and Weder C 2007 Deformation-induced color changes in mechanochromic polyethylene blends *Macromolecules* **40** 2400–8
[20] Chen Y L, Spiering A J H, Karthikeyan S, Peters G W M, Meijer E W and Sijbesma R P 2012 Mechanically induced chemiluminescence from polymers incorporating a 1,2-dioxetane unit in the main chain *Nat. Chem.* **4** 559–62
[21] Neebe M, Rhinow D, Schromczyk N and Hampp N A 2008 Thermochromism of bacteriorhodopsin and its Ph dependence *J. Phys. Chem.* B **112** 6946–51
[22] Durr H A 1990 New photochromic system—potential limitations and perspectives *Pure Appl. Chem.* **62** 1477–82
[23] Schonberg A, Elkaschef M, Nosseir M and Sidky M M 1958 Experiments with 4-thiopyrones and with 2,2′,6,6′-tetraphenyl-4,4′-dipyrylene—the piezochromism of diflavylene *J. Am. Chem. Soc.* **80** 6312–5
[24] Yoshida M, Nakanishi F, Seki T, Sakamoto K and Sakurai H 1997 Two-dimensional piezochromism and orientational modulations in polysilane monolayer *Macromolecules* **30** 1860–2
[25] Davis D A *et al* 2009 Force-induced activation of covalent bonds in mechanoresponsive polymeric materials *Nature* **459** 68–72
[26] Cho S Y, Kim J G and Chung C M 2010 Photochemical crack healing in cinnamate-based polymers *Journal of Nanoscience and Nanotechnology* **10** 6972–6
[27] Bucknall C B and Gilbert A H 1989 Toughening tetrafunctional epoxy-resins using polyetherimide *Polymer* **30** 213–7
[28] Cantwell W J and Morton J 1991 The impact resistance of composite-materials—a review *Composites* **22** 347–62
[29] Allaoui A, Bai S, Cheng H M and Bai J B 2002 Mechanical and electrical properties of a mwnt/epoxy composite *Compos. Sci. Technol.* **62** 1993–8
[30] Bascom W D, Cottington R L, Jones R L and Peyser P 1975 Fracture of epoxy-modified and elastomer-modified epoxy polymers in bulk and as adhesives *J. Appl. Polym. Sci.* **19** 2545–62
[31] Cho S Y, Kim J G and Chung C M 2008 A fluorescent crack sensor based on cyclobutane-containing crosslinked polymers of tricinnamates *Sensors and Actuators B-Chemical* **134** 822–5
[32] Oya N, Sukarsaatmadja P, Ishida K and Yoshie N 2012 Photoinduced mendable network polymer from poly (butylene adipate) end-functionalized with cinnamoyl groups *Polymer Journal* **44** 724–9
[33] Ali A H and Srinivasan K S V 1997 Photoresponsive functionalized vinyl cinnamate polymers: synthesis and characterization *Polymer International* **43** 310–6
[34] Iimura Y, Kobayashi S, Hashimoto T, Sugiyama T and Katoh K 1996 Alignment control of liquid crystal molecules using photo-dimerization reaction of poly(vinyl cinnamate) *IEICE Trans. Electron.* **E79C** 1040–6
[35] Murase S, Kinoshita K, Horie K and Morino S 1997 Photo-optical control with large refractive index changes by photodimerization of poly(vinyl cinnamate) film *Macromolecules* **30** 8088–90
[36] Tsuda M 1964 Some aspects of photosensitivity of poly(vinyl cinnamate) *Journal of Polymer Science Part a-General Papers* **2** 2907
[37] Kim T D, Bae H M and Lee K S 2002 Synthesis and characterization of a new polyester having photo-crosslinkable cinnamoyl group *Bulletin of the Korean Chemical Society* **23** 1031–4
[38] Coleman M M, Hu Y, Sobkowiak M and Painter P C 1998 Infrared characterization of poly(vinyl cinnamate) and its blends with poly(4-vinyl phenol) before and after uv exposure *Journal of Polymer Science Part B-Polymer Physics* **36** 1579–90
[39] Chae B, Lee S W, Ree M, Jung Y M and Kim S B 2003 Photoreaction and molecular reorientation in a nanoscaled film of poly(methyl 4-(methacryloyloxy)cinnamate) studied by two-dimensional ftir and uv correlation spectroscopy *Langmuir* **19** 687–95
[40] Brostow W, Chiu R, Kalogeras I M and Vassilikou-Dova A 2008 Prediction of glass transition temperatures: binary blends and copolymers *Mater. Lett.* **62** 3152–5
[41] Zhou J M and Lucas J P 1999 Hygrothermal effects of epoxy resin. part ii: variations of glass transition temperature *Polymer* **40** 5513–22
[42] Rebizant V, Venet A S, Tournilhac F, Girard-Reydet E, Navarro C, Pascault J P and Leibler L 2004 Chemistry and mechanical properties of epoxy-based thermosets reinforced by reactive and nonreactive sbmx block copolymers *Macromolecules* **37** 8017–27
[43] Sun Y Y, Zhang Z Q, Moon K S and Wong C P 2004 Glass transition and relaxation behavior of epoxy nanocomposites *Journal of Polymer Science Part B-Polymer Physics* **42** 3849–58
[44] Bandyopadhyay A, Valavala P K, Clancy T C, Wise K E and Odegard G M 2011 Molecular modeling of crosslinked epoxy polymers: the effect of crosslink density on thermomechanical properties *Polymer* **52** 2445–52
[45] Blumstei A 1965 Polymerization of adsorbed monolayers.2. thermal degradation of inserted polymer *Journal of Polymer Science Part a-General Papers* **3** 2665
[46] Collier A, Wang H J, Yuan X Z, Zhang J J and Wilkinson D P 2006 Degradation of polymer electrolyte membranes *Int. J. Hydrog. Energy* **31** 1838–54

[47] Chattopadhyay D K and Webster D C 2009 Thermal stability and flame retardancy of polyurethanes *Prog. Polym. Sci.* **34** 1068–133

[48] Aoyagi Y, Yamashita K and Doi Y 2002 Thermal degradation of poly (R)-3-hydroxybutyrate, poly epsilon-caprolactone, and poly (S)-lactide *Polymer Degradation and Stability* **76** 53–9

[49] Starnes W H 2002 Structural and mechanistic aspects of the thermal degradation of poly(vinyl chloride) *Prog. Polym. Sci.* **27** 2133–70

[50] Kim H T and Park J K 1998 Thermal degradation of poly(vinyl cinnamate) *Polym. Bull.* **41** 325–31

[51] Bach R D and Dmitrenko O 2004 Strain energy of small ring hydrocarbons. influence of C-H bond dissociation energies *J. Am. Chem. Soc.* **126** 4444–52